Measurement of beauty production in deep inelastic scattering at HERA

ZEUS Collaboration

S. Chekanov, M. Derrick, J.H. Loizides[1], S. Magill, S. Miglioranzi[1], B. Musgrave, J. Repond, R. Yoshida

Argonne National Laboratory, Argonne, IL 60439-4815, USA [45]

M.C.K. Mattingly

Andrews University, Berrien Springs, MI 49104-0380, USA

N. Pavel

Institut für Physik der Humboldt-Universität zu Berlin, Berlin, Germany

P. Antonioli, G. Bari, M. Basile, L. Bellagamba, D. Boscherini, A. Bruni, G. Bruni, G. Cara Romeo, L. Cifarelli, F. Cindolo, A. Contin, M. Corradi, S. De Pasquale, P. Giusti, G. Iacobucci, A. Margotti, A. Montanari, R. Nania, F. Palmonari, A. Pesci, L. Rinaldi, G. Sartorelli, A. Zichichi

University and INFN Bologna, Bologna, Italy [36]

G. Aghuzumtsyan, D. Bartsch, I. Brock, S. Goers, H. Hartmann, E. Hilger, P. Irrgang, H.-P. Jakob, O. Kind, U. Meyer, E. Paul[2], J. Rautenberg, R. Renner, A. Stifutkin, J. Tandler[3], K.C. Voss, M. Wang

Physikalisches Institut der Universität Bonn, Bonn, Germany [33]

D.S. Bailey[4], N.H. Brook, J.E. Cole, G.P. Heath, T. Namsoo, S. Robins, M. Wing

H.H. Wills Physics Laboratory, University of Bristol, Bristol, United Kingdom [44]

M. Capua, A. Mastroberardino, M. Schioppa, G. Susinno

Calabria University, Physics Department and INFN, Cosenza, Italy [36]

J.Y. Kim, I.T. Lim, K.J. Ma, M.Y. Pac [5]

Chonnam National University, Kwangju, South Korea [38]

M. Helbich, Y. Ning, Z. Ren, W.B. Schmidke, F. Sciulli

Nevis Laboratories, Columbia University, Irvington on Hudson, NY 10027, USA [46]

J. Chwastowski, A. Eskreys, J. Figiel, A. Galas, K. Olkiewicz, P. Stopa, L. Zawiejski

Institute of Nuclear Physics, Cracow, Poland [40]

L. Adamczyk, T. Bołd, I. Grabowska-Bołd [6], D. Kisielewska, A.M. Kowal, M. Kowal,
J. Łukasik, M. Przybycień, L. Suszycki, D. Szuba, J. Szuba [7]

Faculty of Physics and Nuclear Techniques, AGH-University of Science and Technology, Cracow, Poland [47]

A. Kotański [8], W. Słomiński

Department of Physics, Jagellonian University, Cracow, Poland

V. Adler, U. Behrens, I. Bloch, K. Borras, V. Chiochia, D. Dannheim [9], G. Drews,
J. Fourletova, U. Fricke, A. Geiser, P. Göttlicher [10], O. Gutsche, T. Haas, W. Hain,
S. Hillert [11], C. Horn, B. Kahle, U. Kötz, H. Kowalski, G. Kramberger, H. Labes,
D. Lelas, H. Lim, B. Löhr, R. Mankel, I.-A. Melzer-Pellmann, C.N. Nguyen, D. Notz,
A.E. Nuncio-Quiroz, A. Polini, A. Raval, U. Schneekloth, U. Stösslein, G. Wolf,
C. Youngman, W. Zeuner

Deutsches Elektronen-Synchrotron DESY, Hamburg, Germany

S. Schlenstedt

DESY Zeuthen, Zeuthen, Germany

G. Barbagli, E. Gallo, C. Genta, P.G. Pelfer

University and INFN, Florence, Italy [36]

A. Bamberger, A. Benen, F. Karstens, D. Dobur, N.N. Vlasov [12]

Fakultät für Physik der Universität Freiburg i.Br., Freiburg i.Br., Germany [33]

P.J. Bussey, A.T. Doyle, J. Ferrando, J. Hamilton, S. Hanlon, D.H. Saxon, I.O. Skillicorn

Department of Physics and Astronomy, University of Glasgow, Glasgow, United Kingdom [44]

I. Gialas

Department of Engineering in Management and Finance, University of Aegean, Greece

T. Carli, T. Gosau, U. Holm, N. Krumnack, E. Lohrmann, M. Milite, H. Salehi, P. Schleper, T. Schörner-Sadenius, S. Stonjek [13], K. Wichmann, K. Wick, A. Ziegler, Ar. Ziegler

Hamburg University, Institute of Experimental Physics, Hamburg, Germany [33]

C. Collins-Tooth [14], C. Foudas, R. Gonçalo [15], K.R. Long, A.D. Tapper

Imperial College London, High Energy Nuclear Physics Group, London, United Kingdom [44]

P. Cloth, D. Filges

Forschungszentrum Jülich, Institut für Kernphysik, Jülich, Germany

M. Kataoka [16], K. Nagano, K. Tokushuku [17], S. Yamada, Y. Yamazaki

Institute of Particle and Nuclear Studies, KEK, Tsukuba, Japan [37]

A.N. Barakbaev, E.G. Boos, N.S. Pokrovskiy, B.O. Zhautykov

Institute of Physics and Technology of Ministry of Education and Science of Kazakhstan, Almaty, Kazakhstan

D. Son

Kyungpook National University, Center for High Energy Physics, Daegu, South Korea [38]

J. de Favereau, K. Piotrzkowski

Institut de Physique Nucléaire, Université Catholique de Louvain, Louvain-la-Neuve, Belgium

F. Barreiro, C. Glasman [18], O. González, L. Labarga, J. del Peso, E. Tassi, J. Terrón, M. Zambrana

Departamento de Física Teórica, Universidad Autónoma de Madrid, Madrid, Spain [43]

M. Barbi, F. Corriveau, S. Gliga, J. Lainesse, S. Padhi, D.G. Stairs, R. Walsh

Department of Physics, McGill University, Montréal, PQ, H3A 2T8 Canada [32]

T. Tsurugai

Meiji Gakuin University, Faculty of General Education, Yokohama, Japan [37]

A. Antonov, P. Danilov, B.A. Dolgoshein, D. Gladkov, V. Sosnovtsev, S. Suchkov

Moscow Engineering Physics Institute, Moscow, Russia [41]

R.K. Dementiev, P.F. Ermolov, I.I. Katkov, L.A. Khein, I.A. Korzhavina, V.A. Kuzmin, B.B. Levchenko, O.Yu. Lukina, A.S. Proskuryakov, L.M. Shcheglova, S.A. Zotkin

Moscow State University, Institute of Nuclear Physics, Moscow, Russia [42]

I. Abt, C. Büttner, A. Caldwell, X. Liu, J. Sutiak

Max-Planck-Institut für Physik, München, Germany

N. Coppola, G. Grigorescu, S. Grijpink, A. Keramidas, E. Koffeman, P. Kooijman, E. Maddox, A. Pellegrino, S. Schagen, H. Tiecke, M. Vázquez, L. Wiggers, E. de Wolf

NIKHEF and University of Amsterdam, Amsterdam, Netherlands [39]

N. Brümmer, B. Bylsma, L.S. Durkin, T.Y. Ling

Physics Department, Ohio State University, Columbus, OH 43210, USA [45]

A.M. Cooper-Sarkar, A. Cottrell, R.C.E. Devenish, B. Foster, G. Grzelak, C. Gwenlan [19], T. Kohno, S. Patel, P.B. Straub, R. Walczak

Department of Physics, University of Oxford, Oxford, United Kingdom [44]

P. Bellan, A. Bertolin, R. Brugnera, R. Carlin, F. Dal Corso, S. Dusini, A. Garfagnini, S. Limentani, A. Longhin, A. Parenti, M. Posocco, L. Stanco, M. Turcato

Dipartimento di Fisica dell' Università and INFN, Padova, Italy [36]

E.A. Heaphy, F. Metlica, B.Y. Oh, J.J. Whitmore [20]

Department of Physics, Pennsylvania State University, University Park, PA 16802, USA [46]

Y. Iga

Polytechnic University, Sagamihara, Japan [37]

G. D'Agostini, G. Marini, A. Nigro

Dipartimento di Fisica, Università 'La Sapienza' and INFN, Rome, Italy [36]

C. Cormack [21], J.C. Hart, N.A. McCubbin

Rutherford Appleton Laboratory, Chilton, Didcot, Oxon, United Kingdom [44]

C. Heusch

University of California, Santa Cruz, CA 95064, USA [45]

I.H. Park

Department of Physics, Ewha Womans University, Seoul, South Korea

H. Abramowicz, A. Gabareen, S. Kananov, A. Kreisel, A. Levy

Raymond and Beverly Sackler Faculty of Exact Sciences, School of Physics, Tel-Aviv University, Tel-Aviv, Israel [35]

M. Kuze

Department of Physics, Tokyo Institute of Technology, Tokyo, Japan [37]

T. Fusayasu, S. Kagawa, T. Tawara, T. Yamashita

Department of Physics, University of Tokyo, Tokyo, Japan [37]

R. Hamatsu, T. Hirose [22], M. Inuzuka, H. Kaji, S. Kitamura [23], K. Matsuzawa

Tokyo Metropolitan University, Department of Physics, Tokyo, Japan [37]

M. Costa, M.I. Ferrero, V. Monaco, R. Sacchi, A. Solano

Università di Torino and INFN, Torino, Italy [36]

M. Arneodo, M. Ruspa

Università del Piemonte Orientale, Novara, and INFN, Torino, Italy [36]

T. Koop, J.F. Martin, A. Mirea

Department of Physics, University of Toronto, Toronto, ON, M5S 1A7 Canada [32]

J.M. Butterworth [24], R. Hall-Wilton, T.W. Jones, M.S. Lightwood, M.R. Sutton [25],
C. Targett-Adams

Physics and Astronomy Department, University College London, London, United Kingdom [44]

J. Ciborowski [26], R. Ciesielski [27], P. Łużniak [28], R.J. Nowak, J.M. Pawlak, J. Sztuk [29],
T. Tymieniecka, A. Ukleja, J. Ukleja [30], A.F. Żarnecki

Warsaw University, Institute of Experimental Physics, Warsaw, Poland [48]

M. Adamus, P. Plucinski

Institute for Nuclear Studies, Warsaw, Poland [48]

Y. Eisenberg, D. Hochman, U. Karshon, M. Riveline

Department of Particle Physics, Weizmann Institute, Rehovot, Israel [34]

A. Everett, L.K. Gladilin [31], D. Kçira, S. Lammers, L. Li, D.D. Reeder, M. Rosin, P. Ryan, A.A. Savin, W.H. Smith

Department of Physics, University of Wisconsin, Madison, WI 53706, USA [45]

S. Dhawan

Department of Physics, Yale University, New Haven, CT 06520-8121, USA [45]

S. Bhadra, C.D. Catterall, S. Fourletov, G. Hartner, S. Menary, M. Soares, J. Standage

Department of Physics, York University, ON, M3J 1P3 Canada [32]

Abstract

The beauty production cross section for deep inelastic scattering events with at least one hard jet in the Breit frame together with a muon has been measured, for photon virtualities $Q^2 > 2\,\text{GeV}^2$, with the ZEUS detector at HERA using integrated luminosity of 72 pb^{-1}. The total visible cross section is $\sigma_{b\bar{b}}(ep \to e\,\text{jet}\,\mu X) = 40.9 \pm 5.7(\text{stat.})^{+6.0}_{-4.4}(\text{syst.})$ pb. The next-to-leading order QCD prediction lies about 2.5 standard deviations below the data. The differential cross sections are in general consistent with the NLO QCD predictions; however at low values of Q^2, Bjorken x, and muon transverse momentum, and high values of jet transverse energy and muon pseudorapidity, the prediction is about two standard deviations below the data.
© 2004 Published by Elsevier B.V. Open access under CC BY license.

E-mail address: rik.yoshida@desy.de (R. Yoshida).

[1] Also affiliated with University College London, UK.

[2] Retired.

[3] Self-employed.

[4] PPARC Advanced fellow.

[5] Now at Dongshin University, Naju, South Korea.

[6] Partly supported by Polish Ministry of Scientific Research and Information Technology, grant No. 2P03B 12225.

[7] Partly supported by Polish Ministry of Scientific Research and Information Technology, grant No. 2P03B 12625.

[8] Supported by the Polish State Committee for Scientific Research, grant No. 2P03B 09322.

[9] Now at Columbia University, NY, USA.

[10] Now at DESY group FEB.

[11] Now at University of Oxford, UK.

[12] Partly supported by Moscow State University, Russia.

[13] Now at University of Oxford, UK.

[14] Now at the Department of Physics and Astronomy, University of Glasgow, UK.

[15] Now at Royal Holoway University of London, UK.

[16] Also at Nara Women's University, Nara, Japan.

[17] Also at University of Tokyo, Japan.

[18] Ramón y Cajal fellow.

[19] PPARC Postdoctoral Research fellow.

1. Introduction

Deep inelastic scattering (DIS) offers a unique opportunity to study the production mechanism of bottom (b) quarks via the strong interaction in a clean environment where a point-like projectile, a photon with a virtuality Q^2, collides with a proton. Due to the large centre-of-mass energy, $b\bar{b}$ pairs are copiously produced at the electron–proton collider HERA. The large b-quark mass provides a hard scale, making perturbative quantum chromodynamics (QCD) applicable. However, a hard scale can also be given by the transverse jet energy and by Q. The presence of two or more scales can lead to large logarithms in the calculation which can possibly spoil the convergence of the perturbative expansion. Precise differential cross-section measurements are therefore needed to test the theoretical understanding of b-quark production in strong interactions.

The cross sections for b-quark production in strong interactions have been measured in proton–antiproton collisions at the $Sp\bar{p}S$ [1] and the Tevatron [2] and, more recently, in two-photon interactions at LEP [3] and in γp interactions at HERA [4,5]. Some of the b-production cross sections are significantly above the QCD expectations calculated to next-to-leading order (NLO) in the strong coupling constant, α_s.

This Letter reports the first measurement of b-quark production in DIS at HERA, in the reaction with at least one hard jet in the Breit frame [6] and a muon, from a b decay, in the final state:

$$ep \rightarrow eb\bar{b}X \rightarrow e + \text{jet} + \mu + X.$$

In the Breit frame, defined by $\gamma + 2x\boldsymbol{P} = 0$, where γ is the momentum of the exchanged photon, x is the Bjorken scaling variable and $\boldsymbol{P}$ is the proton momentum, a space-like photon and a proton collide head-on. In this frame, any final-state particle with a high transverse momentum is produced by a hard QCD interaction.

In this Letter, a measurement of the visible cross section, $\sigma_{b\bar{b}}$, is presented, as well as several differential cross sections. The measured cross sections are compared to Monte Carlo (MC) models which use leading order (LO) matrix elements, with the inclusion of initial- and final-state parton showers, as well as to NLO QCD calculations. All cross sections are measured in a kinematic region in which the scattered electron, the muon and the jet are well reconstructed in the ZEUS detector.

2. Experimental conditions

The data used in this measurement were collected during the 1999–2000 HERA running period, where a proton beam of 920 GeV collided with a positron or electron beam of 27.5 GeV, corresponding to a centre-of-mass energy of 318 GeV. The total integrated luminosity was (72.4 ± 1.6) pb^{-1}.

A detailed description of the ZEUS detector can be found elsewhere [7,8]. A brief outline of the components that are most relevant for this analysis is given below. The high-resolution uranium-scintillator calorimeter (CAL) [9] consists of three parts: the forward (FCAL), the barrel (BCAL) and the rear (RCAL) calorimeters. Each part is subdivided transversely into towers and longitudinally into one electromagnetic section (EMC) and either one (in RCAL) or two (in BCAL and FCAL) hadronic sections (HAC). The smallest subdivision of the calorimeter is called a cell. The CAL energy resolutions, as measured under test-beam conditions, are $\sigma(E)/E = 0.18/\sqrt{E \text{ (GeV)}}$ for electrons and $\sigma(E)/E = 0.35/\sqrt{E \text{ (GeV)}}$ for hadrons.

Charged particles are tracked in the central tracking detector (CTD) [10], which operates in a magnetic field of 1.43 T provided by a thin superconducting solenoid. The CTD consists of 72 cylindrical drift-chamber layers, organised in nine superlayers covering the polar-angle[49] region $15° < \theta < 164°$. The

transverse-momentum resolution for full-length tracks can be parameterised as $\sigma(p_T)/p_T = 0.0058 p_T \oplus 0.0065 \oplus 0.0014/p_T$, with p_T in GeV.

The position of electrons[50] scattered at small angles to the electron beam direction was measured using the small-angle rear tracking detector (SRTD) [11, 12]. The SRTD is attached to the front face of the RCAL and consists of two planes of scintillator strips, arranged orthogonally. The strips are 1 cm wide and 0.5 cm thick.

The muon system consists of tracking detectors (forward, barrel and rear muon chambers: FMUON [8], B/RMUON [13]), which are placed inside and outside a magnetised iron yoke surrounding the CAL and cover polar angles from $10°$ to $171°$. The barrel and rear inner muon chambers cover polar angles from $34°$ to $135°$.

The luminosity was measured from the rate of the bremsstrahlung process $ep \rightarrow e\gamma p$. The resulting small-angle energetic photons were measured by the luminosity monitor [14], a lead-scintillator calorimeter placed in the HERA tunnel at $Z = -107$ m.

3. Event selection

Events were selected online via a three-level trigger system [8,15]. The trigger required a localised energy deposit in the EMC consistent with that of a scattered electron. At the third level, where a full event reconstruction is available, a muon was required, defined by a track in the CTD loosely matching a track segment in the inner part of the B/RMUON chambers.

The scattered electron candidate was identified from the pattern of energy deposits in the CAL [16]. The energy (E_e) and polar angle (θ_e) of the electron are measured by combining the impact position at the calorimeter with the event vertex. The impact position is measured from the calorimeter cells associated with the electron candidate, but the CTD ($\theta_e < 157°$) and SRTD ($\theta_e > 162°$) detectors are used to improve the measurement whenever the electron trajectory lies within the respective regions of acceptance.

---

[49] The ZEUS coordinate system is a right-handed Cartesian system, with the Z axis pointing in the proton beam direction, referred to as the "forward direction", and the X axis pointing left towards the centre of HERA. The coordinate origin is at the nominal interaction point.

[50] Hereafter "electron" refers both to electrons and positron.

The reconstruction of Q^2 was based on the measurement of the scattered electron energy and polar angle [17]. The Bjorken scaling variables x and y were reconstructed using the Σ-method, which allows the determination of the estimator y_Σ independently of initial state photon radiation by reconstructing the incident electron energy [18].

Events were selected [19] by requiring the presence of at least one muon in the final state and at least one jet in the Breit frame. The final sample was selected in four steps:

(1) *Inclusive DIS event selection*

• a well reconstructed scattered electron was required with energy greater than 10 GeV, $Q^2 > 2$ GeV^2, $y_{JB} > 0.05$ and $y_\Sigma < 0.7$, where y_{JB} is the y variable reconstructed using the Jacquet–Blondel method [20];

• for events with the scattered electron reconstructed within the SRTD acceptance the impact position of the electron was required to be outside a box defined by $|X_e| < 12$ cm and $|Y_e| < 6$ cm. For events without SRTD information, a box cut on the face of the RCAL of $|X_e| < 12$ cm and $|Y_e| < 10$ cm was used. This cut removed electron candidates near the inner edge of the RCAL beampipe hole;

• to reduce the background from collisions of real photons with protons (photo-production), where the scattered electron escapes down the rear beampipe, the variable $E - p_Z$ was required to be in the range $40 < E - p_Z < 65$ GeV. The variable $E - p_Z$ was defined as the difference of the total energy and the longitudinal component of the total momentum, calculated using final-state objects, reconstructed from tracks and energy deposits in the calorimeter;

• the event vertex reconstructed from tracks was required to lie within 50 cm of the nominal interaction point along the beam axis.

(2) *Muon finding*

Muons were identified by requiring a track segment in both the inner and outer parts of the BMUON or RMUON chambers. The reconstructed muons were matched in space and momentum with a track found in the CTD, with a χ^2 probability greater than 1%. This cut rejected the background from muons coming from $K^\pm$ and $\pi^\pm$ decays and from particles produced in hadronic showers in the CAL that may be misidentified as muons. In addition, cuts on the muon momentum, p^μ, the muon transverse momentum, p_T^μ and the

muon pseudorapidity, η^μ, were applied:

• $-0.9 < \eta^\mu < 1.3$ and $p_T^\mu > 2$ GeV corresponding to the BMUON region;

• $-1.6 < \eta^\mu < -0.9$ and $p^\mu > 2$ GeV corresponding to the RMUON region.

The reconstruction efficiency of the muon chambers was calculated separately for BMUON and RMUON using an independent data sample of di-muon events produced in photon–proton collisions [21]. This data sample consisted of elastic and quasi-elastic Bethe–Heitler events ($\gamma\gamma \rightarrow \mu^+\mu^-$) and J/ψ production and it was selected from events triggered by the inner muon chambers. Two tracks, reconstructed in the CTD, with transverse momentum greater than 1 GeV and associated with energy deposits in the CAL consistent with a minimum-ionising particle were required. One of the CTD tracks was required to point to the muon chamber that triggered the event, and the other was used to measure the muon efficiency, defined as the ratio of the number of tracks satisfying the muon matching requirement to the total number of tracks. The measured muon-reconstruction efficiencies are between 20% and 40%, depending on the region of the muon chambers and on the muon transverse momentum.

(3) *Jet finding*

Hadronic final-state objects were boosted to the Breit frame and clustered into jets using the k_T cluster algorithm (KTCLUS) [22] in its longitudinally invariant inclusive mode [23]. The four-momenta of the hadronic final-state objects were calculated from the measured energies and angles, assuming the objects to be massless. The p_T recombination scheme was used. Reconstructed muons were included in the clustering procedure. Events were required to have at least one jet with transverse energy measured in the Breit frame, $E_{T,\text{jet}}^{\text{Breit}}$ above 6 GeV and within the detector acceptance, $-2 < \eta_{\text{jet}}^{\text{lab}} < 2.5$, where $\eta_{\text{jet}}^{\text{lab}}$ is the jet pseudorapidity in the laboratory frame.

(4) *Muon-jet association*

The muons in the sample were associated with the jet containing the corresponding hadronic final-state object using the KTCLUS information. The associated jet was not necessarily the jet satisfying the jet requirements above. To ensure that the associated jet was well reconstructed, it was required to have $E_{T,\text{jet}}^{\text{Breit}} > 4$ GeV.

After these selection cuts, 941 events remained.

4. Monte Carlo simulation and NLO QCD calculations

To correct the results for detector effects and to extract the fraction of events from b decays, two MC simulations were used: RAPGAP 2.08/06 as default and CASCADE 1.00/09 for systematic checks. The predictions of the MC simulations were also compared to the final results.

The program RAPGAP 2.08/06 [24] is an event generator based on leading-order (LO) matrix elements, with higher-order QCD radiation simulated in the leading-logarithmic approximation using initial- and final-state parton showers based on the DGLAP equations [25]. To estimate the background, samples with light and charm quarks in the final state were produced. The process in which a $b\bar{b}$ pair is produced in photon–gluon fusion was used to simulate the signal. The charm and b-quark masses were set to 1.5 GeV and 5 GeV, respectively. The CTEQ5L [26] parameterisation of the proton parton densities was used. Heavy-quark hadronisation was modelled by the Bowler fragmentation function [27]. The rest of the hadronisation was simulated using the Lund string model [28] as implemented in JET-SET 7.4 [29]. The RAPGAP MC includes the LO electroweak corrections calculated using HERACLES 4.6.1 [30].

The CASCADE 1.00/09 MC [31] uses the $O(\alpha_s)$ matrix elements, where the incoming partons can be off-shell. The parton evolution is based on the CCFM equations [32], which are derived from the principles of k_T factorisation and colour coherence. The mass of the b quark was set to 4.75 GeV.

The NLO QCD predictions were evaluated using the HVQDIS program [33,34], which includes only point-like photon contributions. The fragmentation of a b quark into a B hadron was modelled by the Kartvelishvili function [35]. The parameter α was set to 27.5, as obtained by an analysis [36] of e^+e^- data [37]. The semi-leptonic decay of B hadrons into muons was modelled using a parameterisation of the muon momentum spectrum extracted from JETSET, which is in good agreement with measurements made at B factories [38]. This spectrum corresponds to a mixture of direct ($b \to \mu$) and indirect ($b \to c \to \mu$) B-hadron decays. Jets were reconstructed by running the inclusive k_T algorithm, using

the p_T recombination scheme, on the four-momentum of the two or three partons generated by the program. The b-quark mass was set to $m_b = 4.75$ GeV and the renormalisation and factorisation scales to $\mu = \sqrt{p_{T,b}^2 + m_b^2}$, where $p_{T,b}$ is the mean transverse momentum of the b and $\bar{b}$ quarks. The CTEQ5F4 proton parton densities [26] were used. The sum of the branching ratios of direct and indirect decays of B hadrons into muons was fixed to the JETSET 7.4 value of 0.22.

The NLO QCD predictions were multiplied by hadronisation corrections to compare them to the measured cross sections. The hadronisation corrections are defined as the ratio of the cross sections obtained by applying the jet finder to the four-momenta of all hadrons, assumed to be massless, and that from applying it to the four-momenta of all partons. They were evaluated using the RAPGAP program; they lower the NLO QCD prediction by typically 10%.

The uncertainty of the NLO prediction was estimated by varying the factorisation and renormalisation scales, μ, by a factor of 2 and the b-quark mass, m_b between 4.5 and 5.0 GeV and adding the respective contributions in quadrature. Additional uncertainties due to different scale choices and to different fragmentation functions are within the quoted uncertainties. More details of the NLO QCD calculation and of the determination of its uncertainties can be found elsewhere [33,34,39].

5. Extraction of the beauty fraction

A significant background to the process under study is due to muons from in-flight decays of pions and kaons. Such decay muons are mostly characterised by low momenta and, therefore, partly rejected by the cuts $p^\mu > 2$ GeV and $p_T^\mu > 2$ GeV. In addition, the signal reconstructed in the muon chambers can be due to kaons or pions passing through the CAL. Muons can also originate from the semi-leptonic decay of charmed hadrons. These decays produce events topologically similar to those under study.

Due to the large b-quark mass, muons from semi-leptonic b decays usually have high values of the transverse momentum, $p_T^{\rm rel}$, with respect to the axis of the closest jet. For muons from charm decays and
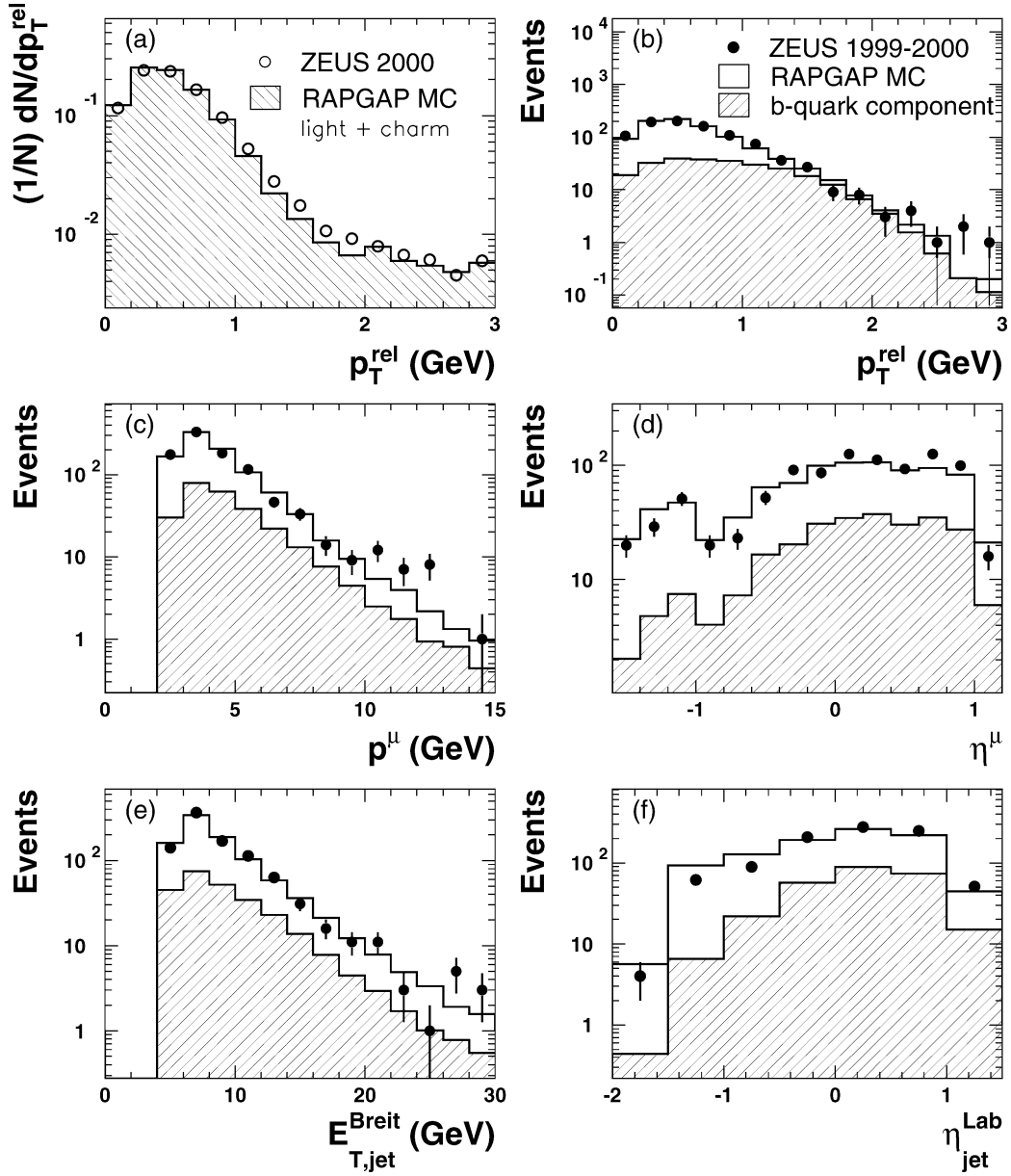
Fig. 1. (a) p_T^{rel} distribution measured for unidentified tracks in an inclusive DIS sample compared with the RAPGAP MC simulation (see text). Data (dots) and the RAPGAP MC (solid line) distributions after the final event selection for: (b) the measured p_T^{rel} distribution; (c) muon momentum; (d) muon pseudorapidity; (e) transverse energy in the Breit frame; and (f) pseudorapidity in the laboratory frame of the associated jet. The solid line represents all MC contributions while the hatched histograms show the contribution from b quarks according to the percentage given by the fit (see Section 7). The error bars are statistical only.

in events induced by light quarks, the p_T^{rel} values are low. Therefore, the fraction of events from b decays in the data sample can be extracted on a statistical ba-

sis by fitting the relative contributions of the simulated bottom, charm and light-quark decays to the measured p_T^{rel} distribution.

The extraction of the fraction of b-quark decays relies on the correct simulation of the shape of the $p_T^{\rm rel}$ distribution for all processes. The simulation was checked with the data. For this purpose, an inclusive DIS data sample with at least one hard jet in the Breit frame was selected, without requiring a muon in the final state. For tracks passing the same selection criteria as required for the muon, the $p_T^{\rm rel}$ distribution was calculated. Fig.1(a) shows the comparison of the shape of the measured $p_T^{\rm rel}$ distribution with the simulated light- and charm-quark contribution. The shape is reasonably well described.

Fig.1(b) shows the measured $p_T^{\rm rel}$ distribution for muon candidates compared to the MC simulation. The MC simulation contains the background processes from light and charm quarks and the contribution from b quarks. The distributions are peaked at low $p_T^{\rm rel}$ values, where the decays of hadrons containing charm and light quarks dominate. At higher $p_T^{\rm rel}$ values, the measured distribution falls less steeply than that expected for light-quark and charm contributions alone. To determine the b-quark fraction in the data, the contributions from light-plus-charm flavours and beauty in the simulation were allowed to vary, and the best fit was extracted using a binned maximum-likelihood method. The measured fraction of events from b decays, f_b, is $(30.2 \pm 4.1)\%$, where the error is statistical. The mixture with the fitted fractions describes the data well.

Fig. 1(c)–(f) shows the comparison between the data and the MC simulation with respect to the momentum and the pseudorapidity of the muon, as well as the associated jet transverse energy in the Breit frame and the pseudorapidity of the associated jet measured in the laboratory frame. The MC simulation, with the different contributions weighted according to the fractions found using the fit procedure described above, reproduces the muon and jet kinematics well.

6. Systematic uncertainties

The systematic uncertainties on the measured cross sections were determined by changing the selection cuts or the analysis procedure in turn and repeating the extraction of the cross sections. The numbers given below refer to the total visible cross section, $\sigma_{b\bar{b}}$. For the differential distributions the systematic uncertain-

Table 1

Single differential b-quark cross sections as functions of Q^2, the Bjorken-x variable, the muon transverse momentum, p_T^μ, the muon pseudorapidity, η^μ, and the transverse energy of the leading jet in the Breit frame, $E_{T,{\rm jet}}^{\rm Breit}$. The statistical and systematic uncertainties are shown separately

Q^2 range (GeV^2)	$d\sigma/dQ^2$ (pb/GeV^2)	$\Delta_{\rm stat}$	$\Delta_{\rm syst}$
2, 10	2.63	± 0.56	$+0.53$ -0.46
10, 40	0.36	± 0.10	$+0.06$ -0.05
40, 1000	0.010	± 0.002	$+0.002$ -0.002
$\log_{10}(x)$ range	da/dx (pb)	$\Delta_{\rm stat}$	$\Delta_{\rm syst}$
$-4.5, -3.5$	20.9	± 4.4	$+3.2$ -3.4
$-3.5, -2.9$	17.2	± 4.7	$+2.3$ -2.5
$-2.9, -1.0$	5.3	± 1.3	$+0.9$ -1.0
p_T^μ range (GeV)	$d\sigma/dp_T^\mu$ (pb/GeV)	$\Delta_{\rm stat}$	$\Delta_{\rm syst}$
2, 3	30.5	± 7.6	$+6.3$ -4.2
3, 4	9.7	± 2.6	$+1.9$ -1.8
4, 15	0.59	± 0.13	$+0.11$ -0.13
η^μ range	$d\sigma/d\eta^\mu$ (pb)	$\Delta_{\rm stat}$	$\Delta_{\rm syst}$
$-1.6, -0.15$	9.1	± 2.2	$+1.9$ -1.5
$-0.15, 0.45$	14.2	± 3.6	$+3.0$ -3.0
0.45, 1.3	19.8	± 4.1	$+3.8$ -3.1
$E_{T,{\rm jet}}^{\rm Breit}$ range (GeV)	$d\sigma/dE_{T,{\rm jet}}^{\rm Breit}$ (pb/GeV)	$\Delta_{\rm stat}$	$\Delta_{\rm syst}$
6, 10	5.7	± 1.4	$+1.4$ -1.3
10, 13	3.4	± 0.8	$+0.5$ -0.4
13, 36	0.40	± 0.08	$+0.05$ -0.05

ties were determined bin-by-bin and are included in the figures and in Table 1. The following systematic studies were carried out:

• selection cuts and SRTD alignment: variation of the selection cuts on data and Monte Carlo by the detector resolution on respective variables (including the electron energy, $E - p_Z$, $E_{T,{\rm jet}}^{\rm Breit}$, $\eta_{\rm jet}^{\rm lab}$ and SRTD box cut). This led to a systematic deviation of $+9.1\%$ and -6.1% with respect to the nominal value, where the biggest uncertainties were introduced by the widened $\eta_{\rm jet}^{\rm lab}$ cut and the increased $E_{T,{\rm jet}}^{\rm Breit}$ cut. The relative alignment between the RCAL and the SRTD detec-

tor is known to a precision of ± 1 mm [40]. The related systematic uncertainty was conservatively estimated by shifting the reconstructed SRTD hit position by ± 2 mm in both coordinates and was $+0.5\%$ and -1.3%, respectively;

• energy scale: the effect of the uncertainty in the absolute CAL energy scale of $\pm 2\%$ for hadrons and of $\pm 1\%$ for electrons was $+3.3\%$ and -0.3%;

• extraction of b decays: the uncertainties related to the signal extraction were estimated by doubling and halving the charm contribution. This leads to a systematic uncertainty of $+5.7\%$ and -3.5%, respectively. The uncertainty obtained by reweighting the light-plus-charm quark $p_T^{\rm rel}$ distribution with the one extracted from the data as described in Section 5 is within this uncertainty;

• muon reconstruction efficiency: the effect of the uncertainty on the muon reconstruction efficiency for the barrel and rear regions of the muon detectors was $+8.9\%$ and -7.8%;

• model dependence of acceptance corrections: to evaluate the systematic uncertainties on the detector corrections, the results obtained with RAPGAP were compared with other MC models: CASCADE; RAPGAP with the Colour Dipole Model [41]; and RAPGAP with the Peterson fragmentation function [42]. Two different values of the ϵ parameter of the Peterson fragmentation function were used, namely $\epsilon = 0.0055$ and 0.0041 as recently determined in $e^+ e^-$ collisions by the SLD and OPAL Collaborations, respectively [43]. The corresponding systematic uncertainty was defined as the maximal deviation with respect to the reference sample and was $+2.2\%$.

These systematic uncertainties were added in quadrature separately for the positive and negative variations to determine the overall systematic uncertainty. These estimates were also made in each bin in which the differential cross sections were measured. The uncertainty associated with the luminosity measurement for the 1999–2000 data-taking periods used in this analysis was $\pm 2.2\%$. This introduces an overall normalisation uncertainty on each measured cross section, which is correlated between all data points. This is added in quadrature to the other systematic uncertainties on the total visible cross section, but is not included in the figures or tables of the differential cross section measurements.

7. Results

The total visible cross section, $\sigma_{b\bar{b}}$, was determined in the kinematic range $Q^2 > 2$ GeV^2, $0.05 < y < 0.7$ with at least one hadron-level jet in the Breit frame with $E_{T,\rm jet}^{\rm Breit} > 6$ GeV and $-2 < \eta_{\rm jet}^{\rm lab} < 2.5$ and with a muon fulfilling the following conditions: $-0.9 < \eta^\mu < 1.3$ and $p_T^\mu > 2$ GeV or $-1.6 < \eta^\mu < -0.9$ and $p^\mu > 2$ GeV. The jets were defined by applying the k_T algorithm to stable hadrons; weakly decaying B (and D) hadrons are considered unstable. The muons coming from direct and indirect b decays are matched to any jet in the event. The measured cross section is

$$\sigma_{b\bar{b}}(ep \to eb\bar{b}X \to e \text{ jet } \mu X)$$
$$= 40.9 \pm 5.7(\text{stat.})^{+6.0}_{-4.4}(\text{syst.}) \text{ pb.}$$

This measurement has been corrected for electroweak radiative effects using HERACLES. The NLO QCD prediction with hadronisation corrections is $20.6^{+3.1}_{-2.2}$ pb which is about 2.5 standard deviations lower than the measured total cross section. The CASCADE MC program gives $\sigma_{b\bar{b}} = 28$ pb and RAPGAP gives $\sigma_{b\bar{b}} = 14$ pb.

The differential cross sections were calculated in the same restricted kinematic range as the total cross section by repeating the fit of the $p_T^{\rm rel}$ distribution and evaluating the electroweak radiative corrections in each bin. The results are summarised in Table 1.

Fig. 2(a) and (b) shows the differential cross sections as functions of Q^2 and x, respectively, compared to the NLO QCD calculation. The NLO QCD predictions generally agree with the data; in the lowest Q^2 and lowest x bins, the data are about two standard deviations higher. Fig. 2(c) and (d) shows the same differential cross sections compared with the RAPGAP and CASCADE MC simulations. CASCADE agrees with the data except for the lowest Q^2 and lowest x bin. RAPGAP is well below the data in all bins, but it reproduces the shapes of the data distributions.

Fig. 3(a) and (b) shows the differential cross sections as functions of the transverse momentum, p_T^μ, and pseudorapidity, η^μ, of the muon, compared to the NLO QCD calculation. They generally agree with the data; in the lowest p_T^μ bin and the high η^μ bin, the NLO QCD prediction is about two standard deviations below the data. Fig. 3(c) and (d) shows the same differential distribution compared with CASCADE and RAPGAP. CASCADE describes the measured cross sections
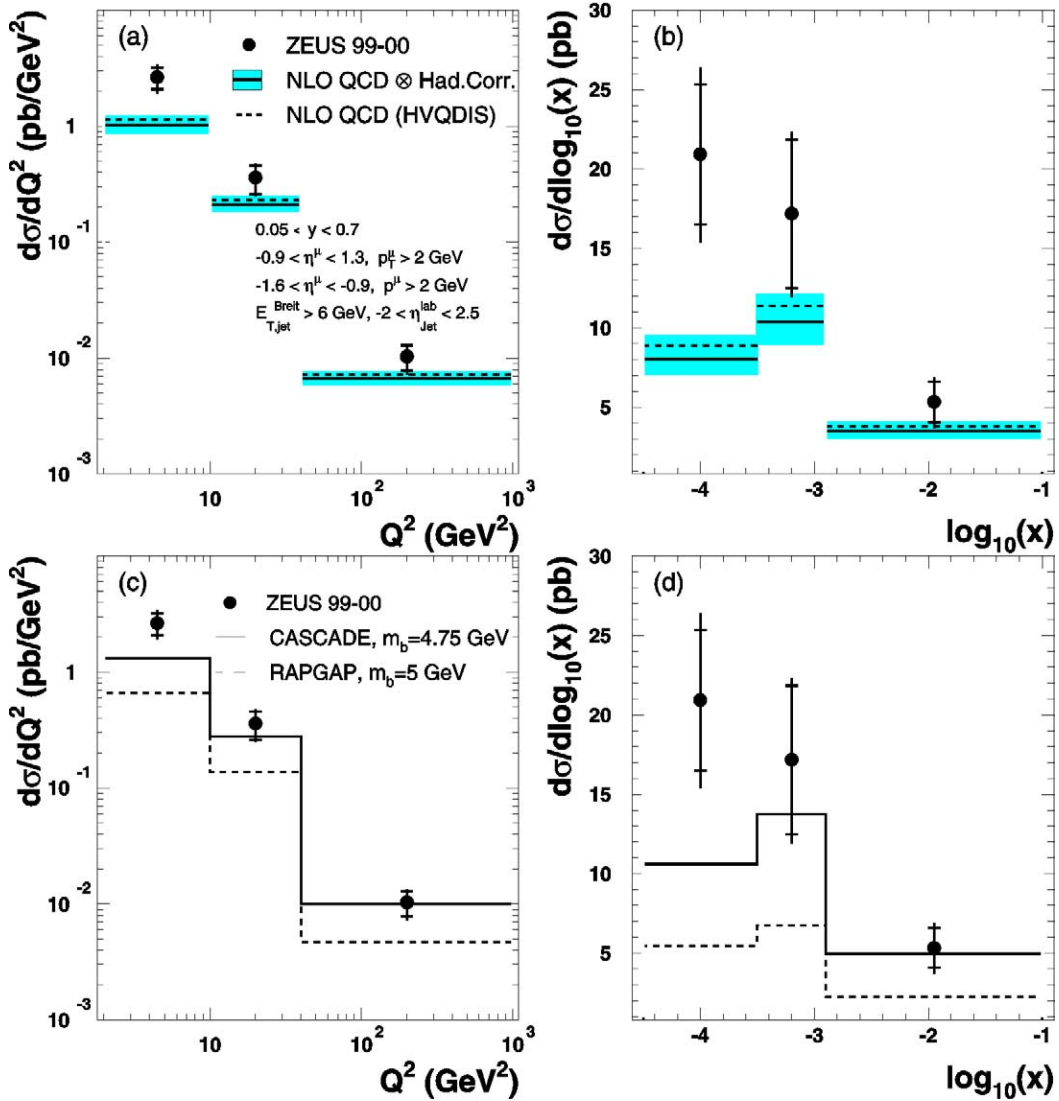
Fig. 2. Differential b-quark cross section as a function of (a) Q^2 and (b) Bjorken x for events with at least one jet reconstructed in the Breit frame and a muon, compared to the NLO QCD calculations. The error bars on the data points correspond to the statistical uncertainty (inner error bars) and to the statistical and systematic uncertainties added in quadrature (outer error bars). The solid line shows the NLO QCD calculations with the hadronisation corrections and the dashed line the same calculation without the hadronisation corrections. The shaded bands show the uncertainty of the NLO QCD prediction due to the variation of the renormalisation and factorisation scale, μ, and the b-quark mass, m_b. Differential b-quark cross sections as a function of (c) Q^2 and (d) Bjorken x, compared with the LO QCD MC programs CASCADE (solid line) and RAPGAP (dashed line).

well except for the lowest p_T^μ bin, while RAPGAP lies below the data.

Fig. 4(a) shows the differential cross section as a function of $E_{T,\text{jet}}^{\text{Breit}}$ of the leading jet compared to the NLO QCD calculation. The NLO QCD prediction agrees with the data reasonably well, though it is sys-

tematically below. For the highest $E_{T,\text{jet}}^{\text{Breit}}$ bin the difference is about two standard deviations. Fig. 4(b) shows the same differential distribution compared with CASCADE and rapgap. For all $E_{T,\text{jet}}^{\text{Breit}}$ values, CASCADE reproduces the measured cross section reasonably well while RAPGAP lies below the data.
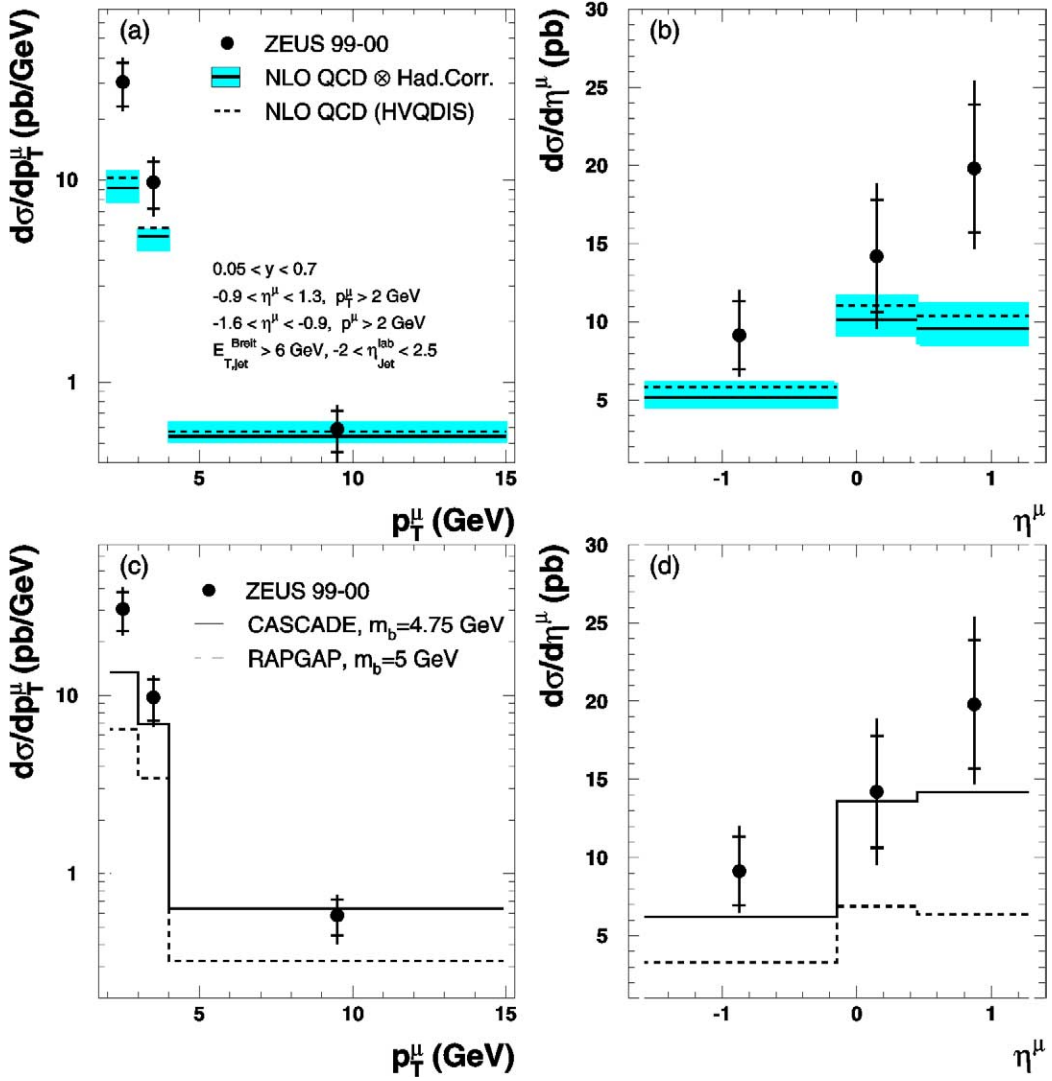
Fig. 3. Differential b-quark cross section as a function of (a) the muon transverse momentum p_T^μ and (b) muon pseudorapidity η^μ in the laboratory frame, compared to the NLO QCD calculations. Other details are as described in the caption to Fig. 2. Differential b-quark cross section as a function of (c) p_T^μ and (d) η^μ, compared with LO QCD MC programs CASCADE (solid line) and RAPGAP (dashed line).

8. Conclusions

The production of b quarks in the deep inelastic scattering process $ep \rightarrow e\mu$ jet X has been measured with the ZEUS detector at HERA. The NLO QCD prediction for the visible cross section lies about 2.5 standard deviations below the measured value.

Single differential cross sections as functions of the photon virtuality, Q^2, the Bjorken scaling variable, x,

the transverse momentum and pseudorapidity of the muon as well as the transverse energy of the leading jet in the Breit frame have been measured. The CAS-CADE MC program, implementing the CCFM QCD evolution equations, gives a good description of the measured cross sections. It is, however, below the data for low values of the transverse momenta, low Q^2 and low values of x. RAPGAP is well below the data for all measured cross sections. The differential cross sec-
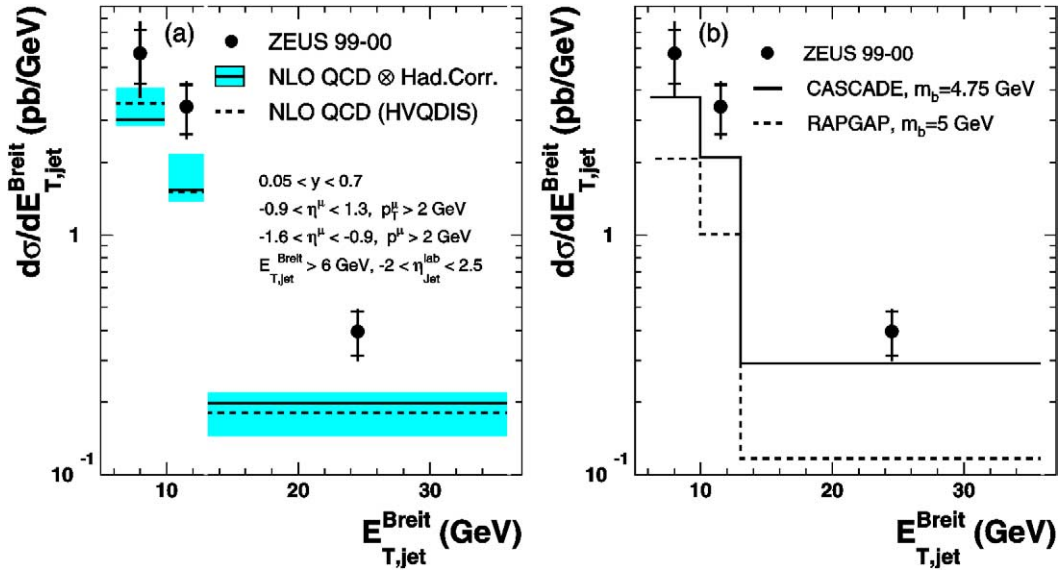
Fig. 4. (a) Differential b-quark cross section as a function of the transverse energy of the jet in the Breit frame $E_{T,\text{jet}}^{\text{Breit}}$. The data (dots) are compared to the NLO QCD calculations (a). Other details are as described in the caption to Fig. 2. (b) Differential b-quark cross sections as a function of $E_{T,\text{jet}}^{\text{Breit}}$ compared with LO QCD MC programs CASCADE (solid line) and RAPGAP (dashed line).

tions are in general consistent with the NLO QCD predictions; however at low values of Q^2, Bjorken x, and muon transverse momentum, and high values of jet transverse energy and muon pseudorapidity, the prediction is about two standard deviations below the data.

In summary, b-quark production in DIS has been measured for the first time and has been shown to be in general consistent with NLO QCD calculations.

Acknowledgements

References

[1] UA1 Collaboration, C. Albajar, et al., Phys. Lett. B 256 (1991) 121;
UA1 Collaboration, C. Albajar, et al., Phys. Lett. B 262 (1991) 497, Erratum.
[2] CDF Collaboration, F. Abe, et al., Phys. Rev. Lett. 71 (1993) 500;
CDF Collaboration, F. Abe, et al., Phys. Rev. Lett. 71 (1993) 2396;
CDF Collaboration, F. Abe, et al., Phys. Rev. D 53 (1996) 1051;
CDF Collaboration, F. Abe, et al., Phys. Rev. D 55 (1997) 2546;
D0 Collaboration, B. Abbott, et al., Phys. Lett. B 487 (2000) 264.
[3] L3 Collaboration, M. Acciarri, et al., Phys. Lett. B 503 (2001) 10.
[4] H1 Collaboration, C. Adloff, et al., Phys. Lett. B 467 (1999) 156;
H1 Collaboration, C. Adloff, et al., Phys. Lett. B 518 (2001) 331, Erratum.
[5] ZEUS Collaboration, J. Breitweg, et al., Eur. Phys. J. C 18 (2001) 625;
ZEUS Collaboration, S. Chekanov, et al., hep-ex/0312057.
[6] R.P. Feynman, Photon–Hadron Interactions, Benjamin, New York, 1972.
[7] ZEUS Collaboration, M. Derrick, et al., Phys. Lett. B 293 (1992) 465.

[8] ZEUS Collaboration, U. Holm (Ed.), The ZEUS Detector. Status Report (unpublished), DESY (1993), available on http://www-zeus.desy.de/bluebook/bluebook.html.

[9] M. Derrick, et al., Nucl. Instrum. Methods A 309 (1991) 77;
A. Andresen, et al., Nucl. Instrum. Methods A 309 (1991) 101;
A. Caldwell, et al., Nucl. Instrum. Methods A 321 (1992) 356;
A. Bernstein, et al., Nucl. Instrum. Methods A 336 (1993) 23.

[10] N. Harnew, et al., Nucl. Instrum. Methods A 279 (1989) 290;
B. Foster, et al., Nucl. Phys. B (Proc. Suppl.) 32 (1993) 181;
B. Foster, et al., Nucl. Instrum. Methods A 338 (1994) 254.

[11] A. Bamberger, et al., Nucl. Instrum. Methods A 401 (1997) 63.

[12] ZEUS Collaboration, S. Chekanov, et al., Eur. Phys. J. C 21 (2001) 443.

[13] G. Abbiendi, et al., Nucl. Instrum. Methods A 333 (1993) 342.

[14] J. Andruszków, et al., Preprint DESY-92-066, DESY, 1992;
ZEUS Collaboration, M. Derrick, et al., Z. Phys. C 63 (1994) 391;
J. Andruszków, et al., Acta Phys. Pol. B 32 (2001) 2025.

[15] W.H. Smith, K. Tokushuku, L.W. Wiggers, in: C. Verkerk, W. Wojcik (Eds.), Proc. Computing in High-Energy Physics (CHEP), CERN, Geneva, Switzerland, 1992, p. 222.

[16] H. Abramowicz, A. Caldwell, R. Sinkus, Nucl. Instrum. Methods A 365 (1995) 508;
R. Sinkus, T. Voss, Nucl. Instrum. Methods A 391 (1997) 360.

[17] S. Bentvelsen, J. Engelen, P. Kooijman, in: W. Buchmüller, G. Ingelman (Eds.), Proc. Workshop on Physics at HERA, vol. 1, DESY, Hamburg, Germany, 1992, p. 23.

[18] U. Bassler, G. Bernardi, Nucl. Instrum. Methods A 361 (1995) 197.

[19] V. Chiochia. PhD thesis, Hamburg University (2003), DESY-THESIS-2003-031.

[20] F. Jacquet, A. Blondel, in: U. Amaldi (Ed.), Proceedings of the Study for an ep Facility for Europe, Hamburg, Germany, 1979, p. 391, also in preprint DESY 79/48.

[21] M. Turcato, PhD thesis, Padova University (2002), DESY-THESIS-2003-039.

[22] S. Catani, et al., Nucl. Phys. B 406 (1993) 187.

[23] S.D. Ellis, D.E. Soper, Phys. Rev. D 48 (1993) 3160.

[24] H. Jung, Comput. Phys. Commun. 86 (1995) 147.

[25] V.N. Gribov, L.N. Lipatov, Sov. J. Nucl. Phys. 15 (1972) 438;
L.N. Lipatov, Sov. J. Nucl. Phys. 20 (1975) 94;
Yu.L. Dokshitzer, Sov. Phys. JETP 46 (1977) 641;
G. Altarelli, G. Parisi, Nucl. Phys. B 126 (1977) 298.

[26] CTEQ Collaboration, H.L. Lai, et al., Eur. Phys. J. C 12 (2000) 375.

[27] M.G. Bowler, Z. Phys. C 11 (1981) 169.

[28] B. Andersson, et al., Phys. Rep. 97 (1983) 31.

[29] T. Sjöstrand, Comput. Phys. Commun. 82 (1994) 74.

[30] A. Kwiatkowski, H. Spiesberger, H.-J. Möhring, Comput. Phys. Commun. 69 (1992) 155.

[31] H. Jung, G.P. Salam, Eur. Phys. J. C 19 (2001) 351, the version 1.00/09 of the program is used;
H. Jung, Comput. Phys. Commun. 143 (2001) 100.

[32] M. Ciafaloni, Nucl. Phys. B 296 (1988) 49;
S. Catani, F. Fiorani, G. Marchesini, Phys. Lett. B 234 (1990) 339.

[33] B.W. Harris, J. Smith, Phys. Rev. D 57 (1998) 2806.

[34] B.W. Harris, J. Smith, Nucl. Phys. B 452 (1995) 109;
B.W. Harris, J. Smith, Phys. Lett. B 353 (1995) 535.

[35] V.G. Kartvelishvili, A.K. Likhoded, V.A. Petrov, Phys. Lett. B 78 (1978) 615.

[36] M. Cacciari, P. Nason, Phys. Rev. Lett. 89 (2002) 122003.

[37] ALEPH Collaboration, A. Heister, et al., Phys. Lett. B 512 (2001) 30.

[38] Belle Collaboration, K. Abe, et al., Phys. Lett. B 547 (2002) 181;
BaBar Collaboration, B. Aubert, et al., Phys. Rev. D 67 (2003) 031101.

[39] T. Carli, V. Chiochia, K. Klimek, JHEP 0309 (2003) 070.

[40] F. Goebel, PhD thesis, University of Hamburg (2001), DESY-THESIS-2001-049.

[41] G. Gustafson, U. Pettersson, Nucl. Phys. B 306 (1988) 746;
B. Andersson, et al., Z. Phys. C 43 (1989) 625.

[42] C. Peterson, et al., Phys. Rev. D 27 (1983) 105.

[43] SLD Collaboration, F. Abe, et al., Phys. Rev. D 65 (2002) 092006;
OPAL Collaboration, G. Abbiendi, et al., Eur. Phys. J. C 29 (2003) 463.